

Synthesis of Highly Ordered Crystalline Wurtzite (ZnO) Membrane for Selenium-Chromium Separation

Sh. Labib and N.A. Tadros

Nuclear Chemistry Department, Hot laboratories Center, Atomic Energy Authority, P.O.Box 13759, Cairo, Egypt, Email: dr_sh_labib@yahoo.com.

تكوين غشاء رقيق من بلورات أكسيد الزنك عالية التنظيم لفصل السيلينيوم والكروميوم

شيراز لبيب ونادية تادروس

ملخص: في هذا البحث تم تحضير كل من أكسيد الخارصين و مركب أكسيد الخارصين- أكسيد السيريوم كطبقات رقيقة مطلاة على دعامات مصنعة من أكسيد التيتانيوم باستخدام طريقة المحلول الهلامي في ظروف تحضير محكمة و ذلك لفصل عنصري الكروم و السيلينيوم. تم تحضير أغشية ذات الطور الثابت (wurtzite) و الشكل المنتظم كما أثبتت دراسات حيود أشعة سينية والمجهر الإلكتروني الماسح. و قد لوحظ وجود زيادة في حجم جسيمات الأغشية المحضرة بزيادة نسبة أكسيد السيريوم المضاف من (1.25 إلى 3 ميكرومل) مما يوضح الدور الفعال لهذا الأكسيد في زيادة تحسين السلوك البلوري للأغشية المحضرة. تم عمل دراسة مفصلة على خصائص الفصل للأغشية المختارة على عنصري الكروم والسيلينيوم. ومن هذه الدراسة تم فصل عنصر السيلينيوم بنسبة عالية مقارنة بعنصر الكروم. ومن ثم نستنتج الدور الكبير والفعال لكل من السلوك القطبي لأكسيد الخارصين في فصل عنصر السيلينيوم والخواص المسامية للأغشية المحضرة في مرور عنصر الكروم خلالها.

ABSTRACT: Pure ZnO and composite ZnO-CeO₂ coated thin films on titania substrates were prepared using a chelating sol-gel method under controlled conditions to be used in the separation and/or rejection of Se(IV) and Cr(VI). XRD and SEM studies confirmed the formation of highly ordered arrays of crystalline wurtzite microstructure with mixed orientation. An increase in average particle size of the prepared membranes from 1.25 to 3 μm with increasing CeO₂ percent was observed indicating the vital role of CeO₂ as secondary phase in improving the crystallinity of the coated films formed. Detailed study of the separation performance of the selected membranes toward Se(IV)-Cr(VI) was studied. A high separation performance for the different membranes prepared was observed toward Se(IV) with respect to Cr(VI). The polar characteristic of ZnO thin films played an essential role in Se(IV) separation. However, a high permeation flow of Cr(VI) through the membranes was governed by the capillary pressure induced within the porous structure of the membranes.

KEYWORDS: Rutile substrate; Pure and composite ZnO membranes; Polymeric sol-gel; SeIV separation; CrVI permeation.

1. Introduction

Heavy metals discharged into the environment from various industries constitute one of the major causes of water and soil pollution (Oboh and Aluor, 2008) and in turn, their presence and accumulation have a toxic effect on human, animal and plant life. (Oboh and Aluor, 2008). Selenium and chromium, as examples of heavy metals, contain undesired properties that affect humans and environments. Selenium, when it is present in the form of seleno-proteins, is an essential element to human nutrition. Moreover, as inorganic, Se(IV), Se(VI) and SeCn⁻ are very toxic to wildlife (Cafferky *et al.* 2006). Chromium naturally occurring as trivalent Cr(III) is an essential nutrient, necessary to life, while hexavalent chromium Cr(VI) is known to be highly toxic; its compounds are highly soluble in water, and carcinogenic in mammals. Commercially, Cr(VI) is available in the form of potassium chromate and potassium dichromate (Jeyasingh and Philip, 2005).

Membrane processes are one of the most efficient methods used to remove toxic elements due to the simplicity in treatment (Saffag *et al.* 2004), higher selectivity and permeability, excellent chemical, thermal and mechanical stability under operating conditions, low maintenance and defect free production (Chen, 2002). Owing to its specific chemical, surface and microstructural properties, ZnO has many industrial applications such as the production of adhesive tapes, automotive tires, ceramics, glasses, varistors, gas sensors, SAW devices, and catalyst and transparent electrodes (Roy and Basu, 2002). So, ZnO is considered to be a promising material to be studied as a ceramic membrane.

This paper deals with the preparation of pure ZnO and composite ZnO-CeO₂ ceramic membranes to remove or separate Se(IV) and Cr(VI) elements from their aqueous solutions using a chelating sol-gel process (Guizard *et al.* 1999). In general the sol-gel process provides a simple method used for the preparation of inorganic membranes with high thermal and chemical stability, controlled microstructure and uniform pore size (Srinivasan and Kumar 2006; Xomeritakis *et al.* 2003). Highly crystalline and crack free films of pure ZnO and composite ZnO-CeO₂ ceramic membranes deposited over porous ceramic substrates were prepared under controlled parameters of processing. Separation performance of the optimized pure and composite ZnO membranes was determined by their higher flux, separation and or rejection toward the toxic elements Se(IV) and Cr(VI).

2. Experimental

2.1 Substrate preparation

Disk rutile substrates of thickness (0.1cm), diameter (10 cm), pore size distribution (0.1-1 μ m) and porosity (55.8 Vol.%) were used for pure ZnO and composite (ZnO-CeO₂) deposition. These substrates were home made from titania powder [Acros rutile powder, 99.5% ,USA]. The starting powder was thermally treated in an air oven at 500 °C for 30 min before any treatments, ground in an agate mortar for 30 min, pressed uniaxially at 12 K.N using P.V.A as binders and sintered at 1200 °C/1h (Labib, 2006).

2.2 Membrane preparation

Pure and composite ZnO sols were prepared using zinc nitrate hexahydrate [99% Merck, Germany], cerium (III) nitrate hexahydrate [99.5% Alpha Aesar, Germany], isopropyl alcohol [99.8% Scharlau, Spain], acetylacetone [\geq 99% Merck, Germany] and distilled water. All the reagents used were A.R. grade. The molar ratio of the precursors used and the composition of the samples prepared are shown in Table 1. Polymeric zinc oxide sol was prepared by drop-wise addition of an alcoholic mixture of isopropyl alcohol (5 mol) and distilled water (0.5 mol) to the stirred alcoholic solution of zinc nitrate and acetyl acetone having molar ratio (Isoprop.alc./zinc nitrate /acetyl acetone) 10:0.5:2 respectively. Otherwise, the different composite zinc oxide-cerium oxide sols were prepared by adding 10, 30 and 50% cerium nitrate to each of the alcoholic solutions of 90, 70 and 50% zinc nitrate, followed by adding acetyl acetone. (Isoprop.alc./zinc nitrate-cerium nitrate/acetyl

acetone: 10:0.5:2). The mixed polymeric sols were prepared by drop-wise hydrolysis with the alcoholic mixture of isopropyl alcohol and distilled water.

Table 1. Optimized precursor's molar ratios and the composition of the different samples.

	Metal Salt [M]	Isopropyl Alcohol [M]	Acetyl Acetone [M]	Distilled Water [M]
	0.5	15	2	0.5
Sample	ZnO %	CeO ₂ %		
100z	100	0		
90z	90	10		
70z	70	30		
50z	50	50		

The different prepared polymeric sols were stirred vigorously for 20 min. The dip coat process was performed at room temperature by immersing rutile substrates into the different prepared polymeric sols for 24h (immersion and withdrawal rate: 0.5mm/s). After dip coating, the different ceramic membranes were left overnight to dry at room temperature. The prepared membranes as well as the different prepared polymeric sols were then dried at 200 °C/1h with a heating and cooling rate of 4°C/min. The process of dipping, withdrawing and drying was repeated 4 times to obtain a suitable coating thicknesses and to repair any defects in the first coating layer (Sekulic *et al.* 2006). Finally, both the supported and unsupported membranes were sintered at 500 °C/1h with a heating and cooling rate of 4 °C/min.

2.3 Membrane characterization

The crystal structures of the different prepared membranes were identified using X-ray diffraction XRD (Philips X'pert multi-purpose diffractometer). A copper-tube x-ray tube operating at 40 KV and 30Ma was used, and the wavelength λ_{Cu} used was 1.54056 Å. The scan was performed over the range 2θ (5-80). The identification of the crystalline phases present was done using the JCPDS database cards. The microstructures and coating thicknesses of the prepared membranes were studied using a scanning electron microscope SEM (JEOL JEM-1200 EX II, made in Japan). Prior to SEM analysis the samples were sputtered with a thin layer of gold using JEOL Fine Coat model JFC-1100E Ion Sputter.

2.4 Membrane performance studies

The most suitable membranes were selected for the separation of the mixed and individual selected heavy metals (SeI(V) and Cr(VI) from their solutions. Synthetic solutions of 100, 50 and 10 ppm of both Se(IV) and Cr(VI) were prepared from selenium oxide (99.9% Sigma-Aldrich, Germany) and potassium dichromate (99.5% ADWIC, Egypt) respectively. The separation experiments were conducted at room temperature under atmospheric pressure, and the selected membranes of an area 0.0314 m² were placed inside a home-made cross flow tubular filtration apparatus made from glass. The cross flow tubular filtration apparatus was adjusted in the vertical position such that the ceramic membranes could be held inside its inner diameter as marked by the grey arrow in Figure 1. This position allowed a uni-directional flow of the feed solution from the ceramic support toward the external ceramic membrane surface. After each run, the membranes were washed several times with distilled water and isopropyl alcohol.

The separation permeability of the ceramic membranes was determined in terms of rejection coefficient R or separation coefficient S that was calculated as a percentage according to Eq. (1) (Yang *et al.* 1998):

$$S = (1 - C_p / C_f) \times 100 \quad (1)$$

SYNTHESIS OF HIGHLY ORDERED CRYSTALLINE WURTZITE (ZnO) MEMBRANE

Where, C_p is the heavy metal concentration in the permeate solution and C_f is the heavy metal concentration in the feed solution (Yang *et al.*1998). The concentration of the heavy metal in the permeate solution was measured using an atomic absorption spectrophotometer (MS Spect. Soolar AA, England). Also, the fluxes J of the membranes were determined using Eq. (2) (Idris and Zain, 2006):

$$J = V/A.\Delta t \quad (2)$$

Where, V is the permeate volume (L), A is the membrane area (m²) and Δt is the permeation time (hour) (Idris and Zain, 2006).

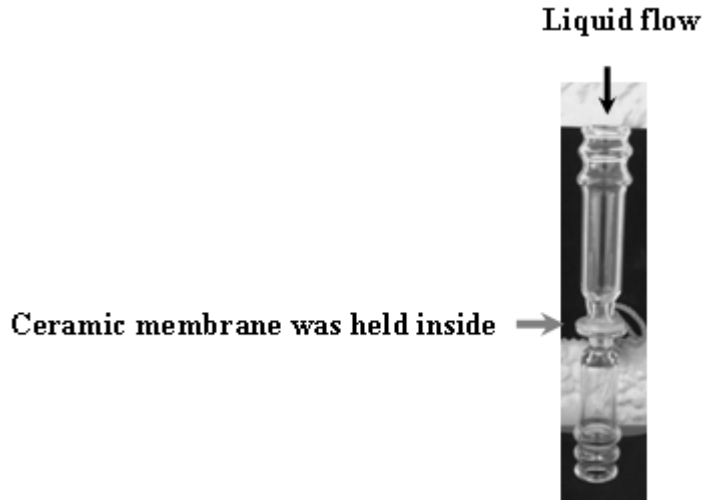


Figure 1. Cross flow tubular filtration apparatus used in the separation experiments.

The selectivity coefficient S was defined as the ratio of initial fluxes for heavy metal 1 and heavy metal 2 respectively, as given in Eq. (3) (Kozłowski *et al.* 2002):

$$S = J_{M1}/J_{M2} \quad (3)$$

3. Results and discussion

3.1 Structural properties

Figure 2 shows the XRD patterns of pure ZnO and composite ZnO-CeO₂ membranes thermally treated at 500 °C/1h. The intensities of the given wurtzite peaks were very low because the films obtained were very thin as shown in the SEM investigations given in Figure 5. Minor diffraction peaks of the wurtzite structure were identified at scattering angles 2θ (56.83, 62.75, 72.5, 76.79) corresponding to the basal planes (110, 103, 201, 004) respectively. X-ray patterns matched the patterns of polycrystalline wurtzite (JCPDS Card no. 03-0888) with unit cell parameters, $a = b = 3.2489\text{\AA}$ and $c=5.2\text{\AA}$ (Kenanakis *et al.* 2007). The crystalline rutile phase was identified (JCPDS Card no. 84-1283) with unit cell parameters, $a = b = 4.593\text{\AA}$ and $c = 2.958\text{\AA}$ respectively. The strongest diffraction patterns of the rutile phase existed at 2θ (27.5, 36.11, 41.27 and 54.5) corresponding to the basal planes (110, 101, 111, 211) respectively. The sharpness of the diffraction peaks was a reflection of the high ordered domains and this in turn was clarified by the uniform microstructure of the membranes obtained (Guizard *et al.*1999; Panda *et al.* 2008).

As shown in Figure 2, there was no peak difference between the different membranes prepared. This was due to the lower coating thickness values of the obtained films as outlined previously. No diffraction peaks of CeO_2 phase were observed. CeO_2 phase fluorite structure (JCPDS card no. 75-0076) was clearly observed in the diffraction pattern of the non-supported membrane (50z) as shown in Figure 3. The broadness of the ceria peak is indicative of the presence of smaller size ceria crystallites in the ZnO matrix, (i.e. nano crystallite ceria particles in the ZnO matrix) (Mishra *et al.* 2003).

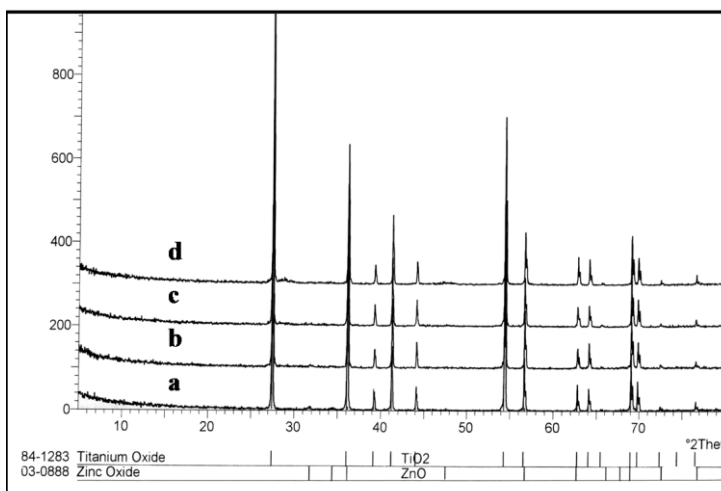


Figure 2. XRD patterns of pure ZnO and composite ZnO- CeO_2 membranes thermally treated at $500^\circ\text{C}/1\text{h}$. (a) 100z, (b) 90 z, (c)70z and (d) 50 z.

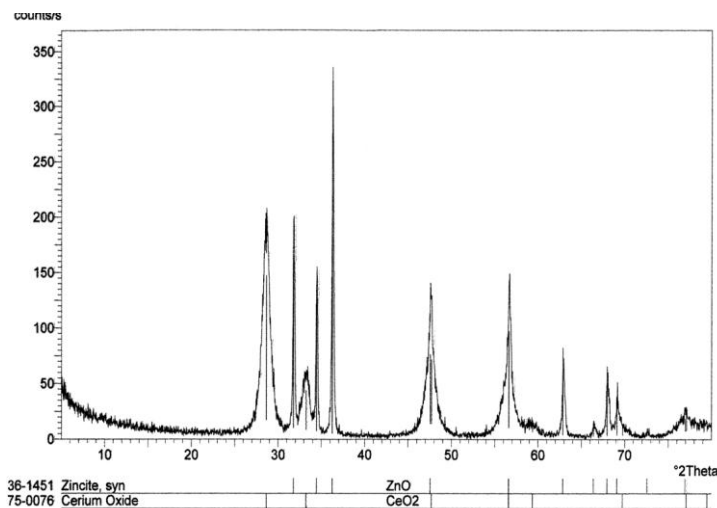


Figure 3. XRD patterns of non supported-membrane 50z thermally treated at $500^\circ\text{C}/1\text{h}$.

The JCPDS card number of the prepared powder 50z was 36-1451, corresponding to pure zincite, which indicated no impurities in the unsupported membranes.

SYNTHESIS OF HIGHLY ORDERED CRYSTALLINE WURTZITE (ZnO) MEMBRANE

3.2 Microstructural Studies

Figures 4 (a-d) show the SEM at a magnification power of 1500x of pure ZnO and composite ZnO-CeO₂ thin films coated over rutile substrates. No variation in particle microstructure was observed in these figures. A continuous hexagonal array of wurtzite particles was shown in the different figures separated by uniform pores. It was observed that no aggregated particles were present. The particle size increased from 1.25 μ m to 1.56 μ m with the addition of 10% CeO₂, see Figures 4 (a-b). A further increase in CeO₂% was accompanied by an increase in particle size to 2.3 μ m and 3 μ m, as shown in Figures 4 (c-d) respectively. The increase of grain size can be attributed to the increased ability of CeO₂ atoms to move toward stable sites in the lattice of ZnO leading to the crystallinity improvement (Öztaş, 2008). An inhomogeneous grain size distribution was observed in sample 70z, Figure 4(c), making it non homogeneous thin film. The average pore diameter values for 100z, 90z and 50z were 0.94, 0.63 and 1.25 μ m respectively as shown in Figures 4 (a, b, d).

Figures 5 (a-d) show the cross SEM of ZnO membranes thermally treated at 500 0C/1h. The fractured coating thicknesses of the different films were very thin and uniform confirming that the bonding strength between the film and the substrate was strong (Hwang *et al.*2005). The coating thicknesses of the different ZnO films deposited were found to be 375 nm for 100z, 1071 nm for 90z, 1428 nm for 70z and 1785 nm for 50z. The increase of the different films coating thickness with increasing CeO₂% means that a fundamental factor impacting the grain size is the increase of coating thickness leading to the decrease of micro-strain and energy band gap in the coated films (Öztaş, 2008).

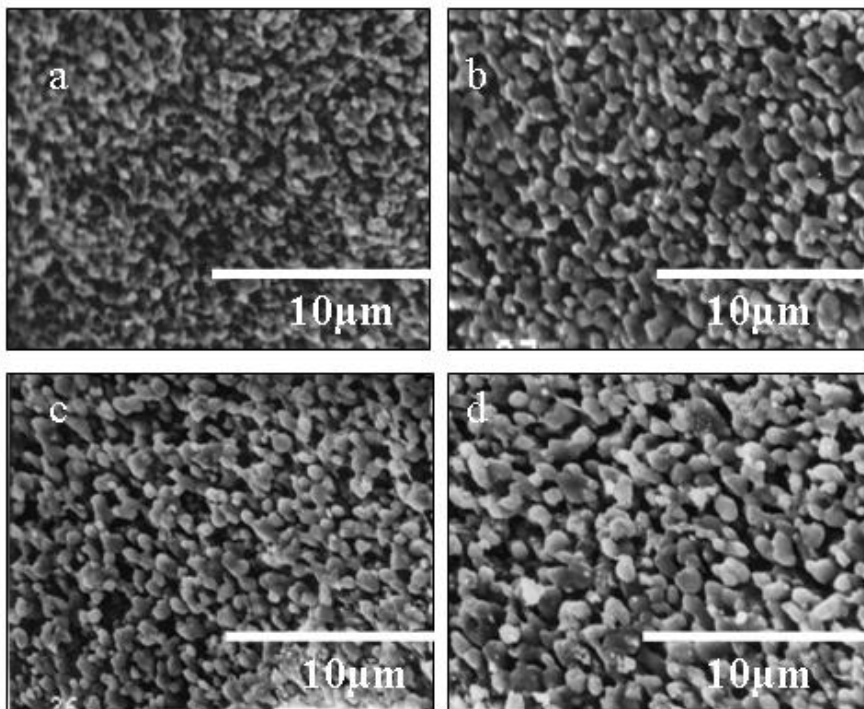


Figure 4. SEM of ZnO membranes thermally treated at 500 0C/1h (a) 100z, (b) 90 z, (c) 70 z and (d) 50 z.

3.3 SeIV-CrVI separation characteristics

The separation studies of Se(IV) and Cr(VI) were performed on the three different membranes 100z, 90z and 50z. High separation rate of Se(IV) values of- 80-90% were obtained through the different membranes as

outlined in Table 2. However very low percentages of Cr(VI) separation were observed through the different membranes. Slight differences in the separation percentage from one membrane to another were due to the characteristic atomic configuration of wurtzite crystal structure, which possesses crystal polarity (Jang *et al.*, 2005; Ban *et al.* 2007). This polarity played an important role in selenium separation, leading to strong interaction between Se particles and ZnO surface charge (Saffag *et al.* 2004). As concluded, the membrane surface charge was significant to the membrane performance, because it affected the electrostatic repulsion between the ions or charged molecules and the membrane surface (Childress and Elimelech, 2000). On the other hand, the high rejection rate of Cr(VI) through the different membranes was governed by the capillary pressure induced within the porous structure of the membranes (Guizard *et al.* 2002).

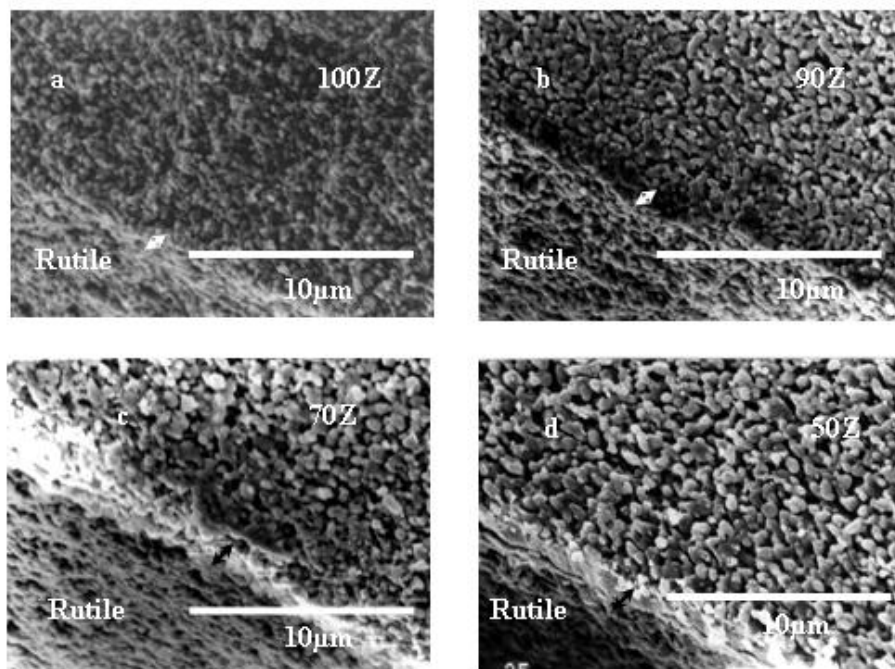


Figure 5. Cross SEM of ZnO membranes thermally treated at 500 °C/1h, magnification 2500 x, (a) 100z, (b) 90 z, (c) 70 z and (d) 50 z.

With a mixture of 100 Se(IV)-50 Cr(VI), a 100% separation rate of Se(IV) and a 100% flow rate of Cr(VI) were observed through the different membranes, as shown in Figure 6. This was due to the increase in the membrane separation performance with the decrease in the effluent concentrations.

Figure 7 shows a decrease in Se(IV) and Cr(VI) flux through the different membranes as a function of Se(IV) and Cr(VI) concentrations. This decrease is explained as follows: the higher the concentration, the higher the osmotic pressure and the lower the permeation flux (Saffag *et al.* 2004). Permeation flux must be proportional to the reciprocal of the membrane thickness, but for a very thin layer, the flux doesn't vary with the thickness of the layer (Byun, 2009). In this case, the flux is controlled by the kinetics of transport through the porous structure and / or the surface exchange reaction (Byun, 2009). Thus the lowest values of Se(IV) flux through the different membranes with respect to Cr(VI) flux were related to the higher separation coefficient of Se(IV) in comparison to Cr(VI) as given previously.

Cr(VI) flux increased with increasing membrane pore diameter as shown in Figure 7b, where the flux order was 50z > 90z > 100z, meaning that wider pore diameter had lesser resistance to Cr transport and so higher flux

SYNTHESIS OF HIGHLY ORDERED CRYSTALLINE WURTZITE (ZnO) MEMBRANE

value. This result confirmed that the transport of Cr(VI) through the different membranes was by the capillary pressure induced within the porous structure of the membranes as outlined before (Guizard *et al.* 2002). The selectivity coefficients for the competitive transport of Cr(VI) and Se(IV) from the prepared aqueous solutions through the membranes used are given in Table 3. The decrease of the selectivity coefficient values for the competitive ions with increasing their concentrations is due to the lower permeation flux at higher concentration (Saffag *et al.* 2004).

Table 2. Se(IV) and Cr(VI) separation coefficient results obtained with the selected membranes.

Membrane type	Average pore diameter (µm)	Average particle size (µm)	Heavy metal concentration	Separation Coefficient for Se(IV)	Separation Coefficient for Cr(VI)
100z 90z 50z	0.94 0.63 1.25	1.25 1.56 3.0	100 ppm	90-92%	2-10 %
100z 90z 50z			50 ppm	≥ 86%	0.1- 2 %
100z 90z 50z			10 ppm	82-86%	0.1-2 %

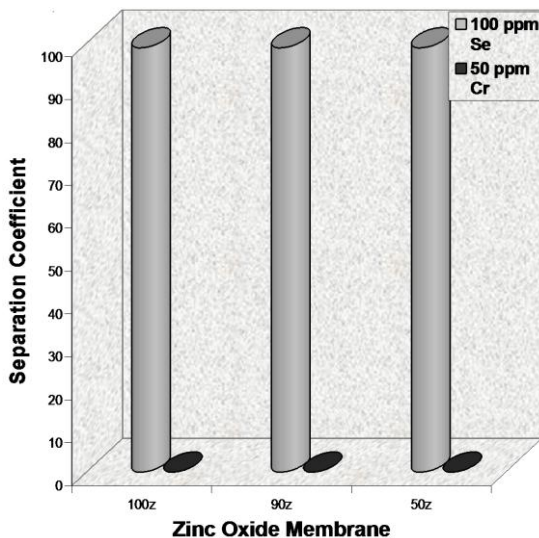


Figure 6. Performance of zinc oxide membranes toward 100Se(IV)-50Cr(VI).

The highest selectivity was obtained through the synthesized membrane 90z. This result is mainly due to its having the narrowest pore size of 90z with respect to the other membranes as shown in Table 2.

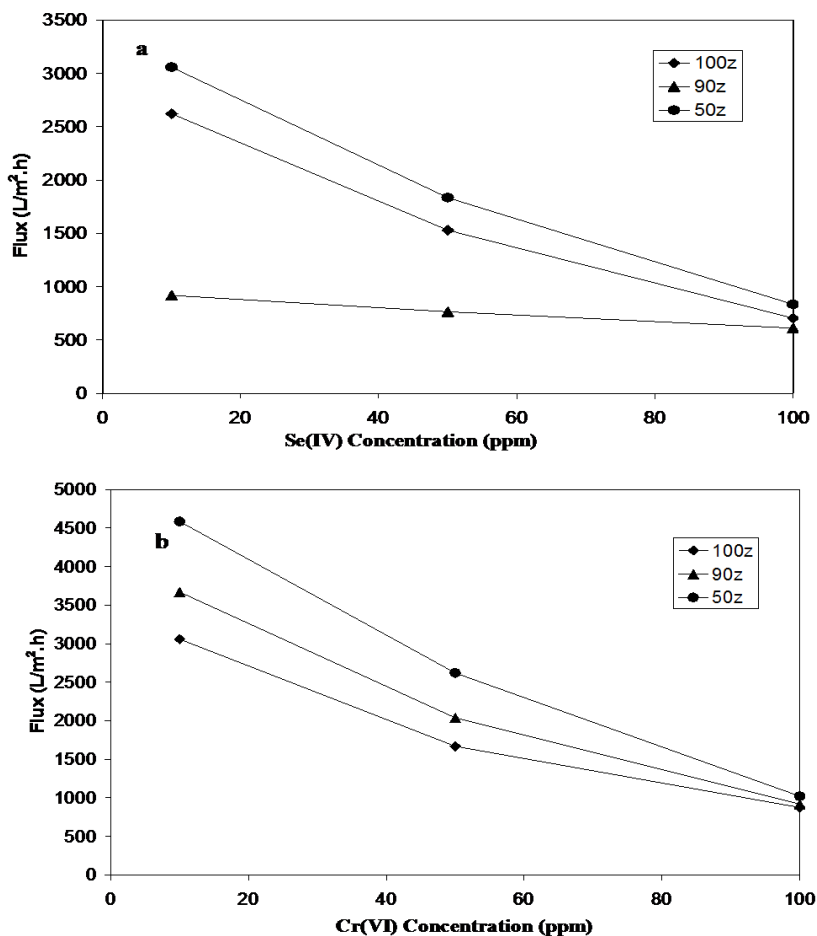


Figure 7. Variation of flux of a - Se(IV) and b - Cr(VI) through different membranes as a function of Se(IV) and Cr(VI) concentrations respectively.

4. Conclusion

The objective of this study was to prepare pure ZnO and composite ZnO-CeO₂ membranes with high permeability to be used in the separation and or rejection of Se(IV) and Cr(VI). Highly ordered hexagonal arrays and crack free thin films of ZnO and ZnO-CeO₂ deposited over titania substrates were prepared using a chelating sol-gel process. The addition of CeO₂ to a ZnO matrix had a great effect on grain size and pore size as well as to the coating thickness of the different films. This result affected the separation performance as well as the selectivity and the flux. A high separation performance for the different membranes prepared was observed toward Se(IV) with respect to Cr(VI). The higher separation rate of Se(IV) was mainly due to the polar characteristic of wurtzite structure. On the other hand, the higher rejection rate of Cr(VI) was governed by the capillary pressure induced by the porous structure of the different membranes selected; the membrane 90z, having the narrowest pore diameter, was characterized by the highest selectivity in comparison to 100z and 50z membranes. So, it is concluded that the ZnO membranes described in this paper show high separation

SYNTHESIS OF HIGHLY ORDERED CRYSTALLINE WURTZITE (ZnO) MEMBRANE

performance and can be used with high accuracy in the separation of Se(IV) from its aqueous solutions. Also, a high separation percentage of Se(IV) from Cr(VI) can be obtained, leading to the decrease of toxicity of any industrial waste containing Se(IV) and Cr(IV) heavy metals.

Table 3. The selectivity coefficient values for the competitive transport of Cr(VI) and Se(IV) through the selected membranes.

Membrane Type	Metal ions concentrations (ppm)		Selectivity Coefficient
	Cr(VI)	Se(IV)	
100z	100	100	1.24
	50	50	1.10
	10	10	1.16
90z	100	100	1.50
	50	50	2.60
	10	10	4.00
50z	100	100	1.20
	50	50	1.40
	10	10	1.50

5. References

- BAN, T., SAKAI, T. and OHYA, Y., 2007. Synthesis of Zinc Oxide Crystals with Different Shapes from Zincate Aqueous Solutions Stabilized with Triethanolamine. *Cryst. Res. Technol.*, **42**: 849-855.
- BYUN, Y.CH., 2009. Oxygen Transport in Ba(Fe, Co, Zr)O_{3-δ}. M.Sc. Thesis, Der Rheinisch-Westfälischen Technischen Hochschule Aachen, Germany.
- CAFFERKY, K.D., RICHARDSON, D.D. and CARUSO, J.A., 2006. ICP-MS Speciation Analysis: Three Roles of Selenium *Spectroscopy*, **21**: 18-24.
- CHEN, J.CH., 2002. Evaluation of Polymeric Membranes for Gas Separation Processes: Poly (Ether-b-Amide) PEPAX Block Copolymer” M.Sc. Thesis, Waterloo University, Ontario, Canada.
- CHILDRESS, A.E. and ELIMELECH, M., 2000. Relating Nanofiltration Membrane Performance to Membrane Charge (Electrokinetic) Characteristics. *Environ. Sci. Technol.*, **34**: 3710-3716.
- GUIZARD, C.G., JULBE, A.C. and AYRAL, A., 1999. Design of Nanosized Structures in Sol-gel Derived Porous solid. *J. Mater. Chem.*, **9**: 55-65.
- GUIZARD, C., AYRAL, A. and JULBE, A., 2002. Potentiality of Organic Solvents Filtration with Ceramic Membranes. A Comparison with Polymer Membranes, *Desalination*, **147**: 275-280.
- HWANG, K.S., JEON, Y.S., KANG, B.A., NISHIO, K., TSUCHIYA, T. and KOR, J., 2005. Crystallinity, Surface Morphology and Optical Properties of Nanocrystalline ZnO Films Prepared with a Metal Naphthenate. *Phys. Soc.*, **46**: 521-526.
- IDRIS, A. and ZAIN, N.M.J., 2006. Effect of Heat Treatment on the Performance and Structural Details of Polyethersulfone Ultrafiltration Membranes. *Teknologi*, **44**: 27-40.
- JANG, K.W., MINEGISHI, T., SUZUKI T., HONG, S.K., OH, D.C., HANADA, T., CHO, M.W. and YAO, T., 2005. Control of Crystal Polarity of ZnO and GaN Epitaxial Layers by Interfacial Engineering. *Ceram. Proc. Res.*, **6**:167-183.
- JEYASINGH, J. and PHILIP, L., 2005. Bioremediation of Chromium Contaminated Soil: Optimization of Operating Parameters Under Laboratory Conditions. *J. Hazard. Mater*, **B118**: 113-120.

- KENANAKIS, G., ANDROULIDAKI, M., KOUDOUMAS, E., SAVVAKIS, C. and KATSARAKIS, N., 2007. Photoluminescence of ZnO Nanostructures Grown by the Aqueous Chemical Growth Technique. *Superlattices and Microstructures*, **42**: 473-478.
- KOZLOWSKI, C., APOSTOLUK, W., WALKOWIAK, W. and KITA, A., 2002. Removal of Cr (VI), Zn, and Cd Ions by Transport Across Polymer Inclusion Membranes with Basic Ion Carriers Physicochemical. *Problems of Mineral Processing*, **36**: 115-122.
- MISHRA, B.G., RAO, G.R. and POONGODI, B., 2003. Hydrogen Transfer Reaction of Cyclohexanone with 2-Propanol Catalyzed by CeO₂-ZnO Material: Promoting Effect of Ceria. *Proc. Indian Acad. Sci. (Chem. Sci.)*, **115**: 561-571.
- OBOH, O.I. and ALUYOR, E.O., 2008. The removal of heavy metal ions from aqueous solutions using sour sop seeds as biosorbent. *African J. of Biotechnology*, **7**: 4508-4511.
- ÖZTAŞ, M.CH., 2008. Influence of Grain Size on Electrical and Optical Properties on InP Films. *Phys. Lett.* **25**: 4090-4092.
- PANDA, S.K., SINGH, N., HOODA J. and JACOB, C., 2008. Growth and luminescence Properties of Large Scale Zinc Oxide Nanotetrapods. *Cryst. Res. Technol.*, **43**: 751-755.
- ROY, S. and BASU, S., 2002. Improved Zinc Oxide Film for Gas Sensor Applications. *Bull. Mater. Sci.*, **25**: 513-515.
- SAFFAG, N., LOUKILI, H., YOUNSSI, S.A., ALBIZANE, A., BOUHRIA, M., PERSIN, M. and LARBOT, A., 2004. Filtration of Solution Containing Heavy Metals and Dyes by Means of Ultrafiltration Membranes Deposited on Support Made of Moroccan Clay. *Desalination*, **168**: 301-306.
- SEKULIC, J., LUITEN, M.W.J., ELSHOF, J.E.T., BENES, N.E. and KEIZER, K., 2006. Microporous Silica and Doped Silica Membrane for Alcohol Dehydration by Pervaporation. *Desalination*, **148**: 19-23.
- LABIB, SH., 2006. Preparation, Characterization and Formulation of Nanoceramic Materials to be Used for the Separation of Some Heavy Metals. Ph.D. Thesis, Ain Shams Uni., Egypt.
- SRINIVASAN, G. and KUMAR J., 2006. Optical and Structural Characterization of Zinc Oxide Thin Films Prepared by Sol-gel Process. *Cryst. Res. Technol.*, **41**: 893-896.
- XOMERITAKIS, G., BRAUNBARTH, C.M., MARSLY, B.S., LIU, N., KÖHN, R., KLIPOWICZ, Z. and BRINKER, C.J., 2003. Aerosol-Assisted Deposition of Surfactant-templated Mesoporous Silica Membranes on Porous Ceramic Supports. *Microporous and Mesoporous Materials*, **66**: 91-101.
- YANG, C., ZHANG, G., XU, N. and SHI, J., 1998. Preparation and Application in Oil-water Separation of ZrO₂/α-Al₂O₃ MF Membrane. *J. Memb. Sci.*, **142**: 235-243.
-

Received: 26 February 2011

Accepted: 10 December 2011